Thermal conductivity of normal liquid ^{3}He

Dennis S. Greywall
AT&T Bell Laboratories, Murray Hill, New Jersey 07974
(Received 13 October 1983)

The thermal conductivity κ of normal liquid ^{3}He was measured along isochores for $7\ \text{mK} < T \lesssim 1$ K and for $0 < P < 30$ bars. The data, obtained using the standard steady-state heat-flow method, are based on the same temperature scale recently used for specific-heat measurements. They are $\sim 10\%$ smaller than earlier low-temperature results obtained near $P=0$. Extrapolations of the data to $T=0$ are in very good agreement with the s- and p-wave approximation if the most-recently-determined quasiparticle effective mass is used. At very-low temperatures the data are consistent with theory which predicts that at low-but-finite temperature $1/\kappa T$ should have the form $a+bT$. However, contrary to the earlier measurements at $P=0$, the new results clearly indicate that higher-order terms are also significant. With the combination of thermal-conductivity and specific-heat results, values of the scattering time τ_κ were determined. By fitting $1/\tau_\kappa T^2$ to an expression of the form $a_\tau + b_\tau T + c_\tau T^2 \ln(T/\Theta_\tau)$ we found values of the characteristic temperature Θ_τ which agree well with those extracted from the $T^3 \ln T$ correction to the low-temperature specific heat.

I. INTRODUCTION

All of the thermodynamic and transport properties of normal liquid ^{3}He at low temperatures can be determined given the scattering amplitude for two-quasiparticle collisions. Moreover, the interaction between normal-state quasiparticles can be directly related to the interaction between superfluid quasiparticles. Obviously then, a complete theory of liquid ^{3}He would provide a scattering amplitude, based on first principles, which accurately predicted all of the measured properties. A more realistic intermediate goal of theory is to relate the information from thermodynamic measurements, i.e., the Landau parameters, to transport properties and thereby to make inferences about the scattering amplitude. It is clear that theoretical progress from this direction depends directly on accurate and precise experimental data.

A serious problem from the experimental point of view has been the controversy regarding the effective mass m_3^* of the ^{3}He quasiparticles, which is extracted from normal-state specific-heat measurements. This is a crucial quantity since it enters into the determination of all of the Landau parameters. Very recently, however, high-precision specific-heat (C_V) measurements[1] have been made over a very large range of pressure and temperature, and these data have been shown to satisfy several thermodynamic checks. Because the new determination of the mass differs from that used in most of the earlier theoretical calculations, some reanalysis and reevaluation is necessary.

Another deficiency of the experimental situation is that there have been few precise measurements of transport properties. These measurements are generally more difficult, for various reasons, but given recent improvements in experimental techniques, high-quality data are certainly feasible.

Of the transport-property measurements, perhaps the measurement of thermal conductivity is most straightforward since there is little ambiguity or complication in the manner in which the conductivity is extracted from the variables actually measured, namely temperature and power. This is in contrast to, for example, the viscosity as measured using a vibrating-wire viscometer.[2] The difficulties in the measurement of conductivity at very low temperatures arise mainly because of the thermal boundary resistance. As the temperature increases, the problem becomes the rapidly decreasing thermal diffusivity, which implies a rapidly increasing thermal relaxation time. It is presumably for these reasons that few measurements[3–6] of the thermal conductivity of normal liquid ^{3}He have been made. Only one[6] of these sets of data, at $P \approx 0$, extends below 30 mK.

In this paper, thermal-conductivity data are reported which have an order of magnitude greater precision than any of the previous transport-property measurements on normal liquid ^{3}He. The results span the temperature range 7 mK—1 K and the pressure range 0—30 bars. The extrapolations of the data to $T=0$ agree well with theory, provided m_3^* from Ref. 1 is used in the calculations. Even at the lowest temperatures the conductivity data show deviations from $1/T$ behavior. These deviations are consistent with predictions for the leading finite-temperature corrections, but show that higher-order terms also contribute significantly.

II. EXPERIMENTAL DETAILS

A. Thermal-conductivity cells

It was necessary to employ two different thermal-conductivity cells in order to make high-precision measurements over the entire temperature range from 7 mK to 1 K. Figure 1 shows the "low-temperature" cell used only below 50 mK. Figure 2 shows the apparatus used at higher temperatures. Having the two very different designs was predicated on the rapidly changing boundary

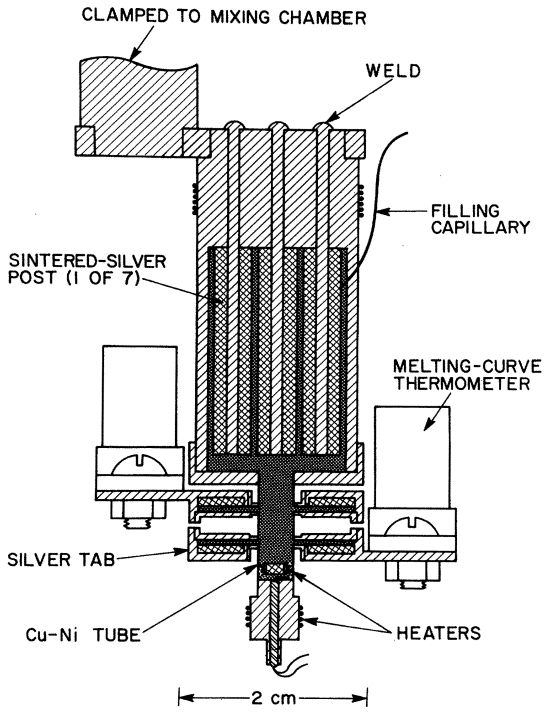

FIG. 1. "Low-temperature" thermal-conductivity cell. This apparatus was used to obtain data between 7 and 50 mK.

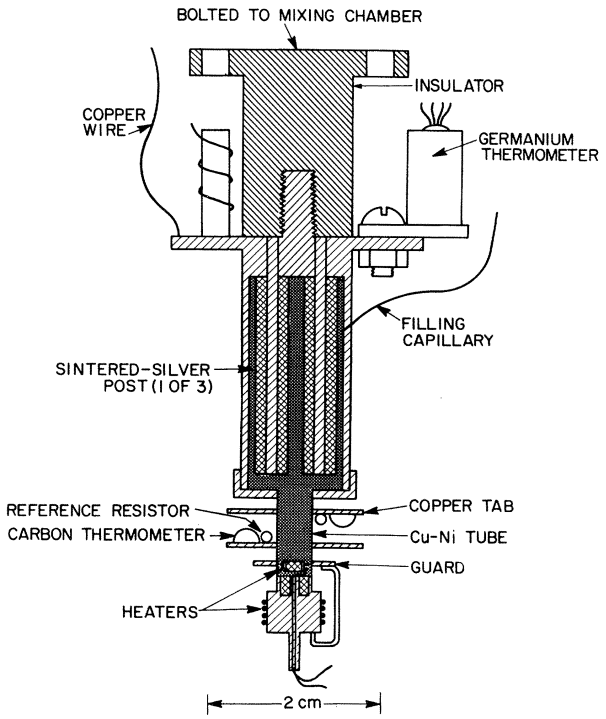

FIG. 2. "High-temperature" thermal-conductivity cell. This apparatus was used to obtain data above 50 mK.

resistance between the normal liquid ^{3}He and its container, the rapidly changing thermal diffusivity of the sample, and also the need for different types of thermometry in the two temperature regimes. Owing to the combination of a very large ^{3}He specific heat and a small thermal conductivity, at all but the very lowest temperatures, both cell lengths were kept short to prevent the thermal time constants from becoming unmanageably long. The tube diameters were taken as a compromise between the conditions that the diameter be (i) small compared to the tube length in order to promote a uniform temperature in planes perpendicular to the tube axis, and (ii) large enough so that the heat generated in the thermometers themselves would not produce a significant temperature gradient along the tube. Since the ^{3}He quasiparticle mean free path is of the order of micrometers at 7 mK, it did not enter into the design considerations. The dimensions of the tubes and other physical parameters of the two apparatuses are listed in Table I.

The upper end of the tube on the low-temperature ap-

TABLE I. Parameters for the thermal-conductivity cells shown in Figs. 1 and 2.

		"Low-T" cell	"High-T" cell
Tube material		Cu_{70}-Ni_{30}	Cu_{70}-Ni_{30}
Tube length (cm)		1.2	1.0
Tube internal diameter[a] (cm)		0.357	0.364
Tube-wall thickness (cm)		0.011	0.0051
Tab spacing[a] (center to center) (cm)		0.394	0.399
Surface area (m^2):	large exchanger	20	10
	tabs	2	
	end plug		0.2
	heater disk	0.02	0.02
Heater resistances (Ω):[b]	inside	330.5	342.4
	outside	1007.6	906.2

[a]Room-temperature values.
[b]Measured at 100 mK.

paratus joined into a heat exchanger with a surface area of ~ 20 m^2. Strong thermal contact between the silver body of this chamber and the mixing chamber of a dilution refrigerator was made using a mechanical clamp (Fig. 1 of Ref. 1). The temperature of the helium at the cold end of the tube was therefore closely tied to the temperature of the mixing chamber, making it possible to extend the range of the data to near the limiting temperature of the refrigerator itself. The Pt-W heater used to generate the temperature gradient in the liquid was supported inside and near the bottom of the tube by its superconducting leads. It was wound around the perimeter of a disk formed by a short thin-walled silver cylinder packed with silver powder (225 cm^2). The disk was intended to reduce the temperature rise of the heater wire and also to promote a heat flow uniformly parallel to the tube axis. Since the thermal conductance of the containment tube was small compared to that of the helium sample, only a small fraction of the heat had to flow across this helium-metal interface. Nevertheless, because of the large thermal boundary resistance at low temperature, and also because of the power dissipated in the thermometers, special care had to be taken to ensure that the temperature measured on the outside of the tube accurately corresponded to the abutting sample temperature. Therefore each of the thermometer tabs soldered to the tube was constructed with an inside surface area of ~ 2 m^2. The helium sample came in contact with the silver sponges via ten 0.75-mm-diam holes drilled radially through the wall of the tube. The temperatures of the tabs were measured using ^{3}He-melting-curve thermometers.[7]

Because of the very long response times at the higher temperatures, this apparatus was useful only below about 50 mK. The long times were primarily a consequence of the large thermal mass of the ^{3}He in the tabs and in the melting-curve thermometers.

At higher temperatures, the apparatus shown in Fig. 2 had a much faster response time. This much simpler cell could be used at these temperatures because of the much smaller boundary resistance, and also because carbon-resistance thermometry becomes reliable and possesses adequate sensitivity. On this apparatus the thermometer tabs were simply thin (0.4-mm-thick) copper disks soft-soldered to the outside of the tube. The tube had a very thin wall (0.05-mm-thick), and thus the correction for the shunting effect of the wall conductance remained small (See Sec. II D), and also, and more importantly, only a small (0.2-m^2) heat exchanger was needed to hold the lowest portion of the sample and bottom end cap at nearly the same temperature. The end cap was epoxied onto the tube, but a heavy copper wire hard-soldered to both pieces guaranteed that they were in good thermal contact. The attachment of the wire to the tube was via a copper disk which was positioned level with the top of the inside heater assembly in an attempt to further reduce temperature differences between the sample and the warm end of the tube. The guard ring also served to strengthen the cell. Since nearly all of the heat had to flow across a liquid-solid interface at the top of the tube, a much larger surface area was needed here to prevent significant temperature differences from developing. The top heat exchanger contained three sintered silver posts with a total surface area of ~ 10 m^2. Attached to the flange welded to this heat exchanger were a calibrated germanium thermometer, a superconducting fixed-point device, and a cerium-magnesium-nitrate thermometer.[7] These thermometers were used to calibrate the carbon resistors on the tabs. A thermally insulating support positioned the cell below the mixing chamber of the refrigerator. Thermal connection to the refrigerator was via a 10-cm-long, 0.06-cm-diam copper wire. This weak link made it possible to accurately control the temperature of the cell at high temperatures. The heater wrapped on the outside of the bottom end plug was used in measuring the conductance of the unfilled tube.

All the samples were confined to constant volume using a valve also attached to the mixing chamber. The valve and the conductivity apparatus were surrounded by a radiation shield at the mixing-chamber temperature.

B. Thermometry

A description and cross-sectional drawing of the ^{3}He-melting-curve thermometers used on the low-temperature cell (Fig. 1) are given in Ref. 7. However, pressure readings were converted to temperatures using the corrected P-T relation from Ref. 1. This calibration of the melting curve used, as partial input, the condition that the ^{3}He specific heat, measured using this type of thermometer, be linear in T at very low temperatures. We now find that this calibration also implies a ^{3}He thermal conductivity at our lowest temperatures which is well behaved and consistent with qualitative theoretical expectations.

The two thermometers, which had a common filling capillary above ~ 0.7 K, were made as identical as possible and had very similar capacitance-versus-pressure relationships. The pressure calibrations were performed simultaneously near 1 K using a dead-weight tester. The reference capacitors used in the ratio-transformer—bridge circuits were carefully shielded 20-pF silver-mica capacitors kept in a liquid-nitrogen bath. With the cell heaters turned off, the two thermometers registered the same temperature to within $0.001\,T$, and showed no detectable relative drifts when monitored for periods of several hours. At a bridge excitation of 2 V rms, the power dissipated in each of the thermometers was 2×10^{-11} W. This power level was always less than $\sim 0.1\%$ of the power used to generate the temperature gradients along the cell. This power level also caused an estimated temperature difference across the helium-silver boundary in the tabs of about 1 μK at 7 mK.

The melting-curve thermometers have sufficient resolution to measure temperature differences of $\sim 0.06T$ to within a precision of better than 0.2%. The scatter in the data is somewhat larger at very low temperatures because of difficulties in regulating the temperature at a level of the thermometer resolution. Between roughly 20 and 50 mK, additional uncertainty is attributable to the very long thermal time constants in the low-temperature apparatus; near 50 mK it was necessary to wait 5 or 6 h for a steady state to be reestablished after switching the heater on.

The carbon-resistance thermometry used on the high-temperature cell is similar to that described in Ref. 8. In

the present experiment the thermometers were 220-Ω, 0.5-W Speer resistors which were ground to a thickness of about 0.25 mm. The reference resistors were 10-kΩ metal-film resistors also varnished onto the copper tabs. Below 200 mK the bridge driving voltage was 250 μV, which gave a temperature resolution of better than $2\times10^{-4}T$. At higher temperatures the driving voltage was increased to 630 μV. The power dissipated in the thermometers and reference resistors was always negligible compared to that dissipated in the cell heater.

C. Measurement of thermal conductivity

The thermal-conductivity measurements were made using the conventional technique: Heat was forced to flow through the sample by dissipating power $\dot{Q}$ in the resistor located very near the bottom of the sample. The resulting equilibrium temperature difference ΔT between the two tabs was then measured and related to the thermal conductivity κ at the mean temperature via the expression

$$\dot{Q}=-\kappa A\Delta T/\Delta x \ . \tag{1}$$

Here A is the cross-sectional area of the sample and Δx is the spacing between the thermometers. The heat was forced to flow upward because of the negative expansion coefficient of normal liquid ^{3}He at low temperature; heating from the top would have easily caused convective flow.

Because the conductivity cells (Figs. 1 and 2) are relatively short and the thickness of the thermometer tabs is a sizable fraction of their separation, special attention has to be given to the determination of the effective thermometer spacing. On the high-temperature cell the tabs are copper disks soft-soldered to the outside of the tube. Although copper has a high conductivity, the tabs do not shunt the flow of heat in Cu-Ni tube because of the thermal separation provided by the ring of soft solder. The temperature of each disk should then be very close to the average temperature of the abutting section of the tube. Thus, to a good approximation, Δx for this cell is equal to the center-to-center spacing of the tabs.

For the low-temperature cell the situation is more complicated. Since the helium sample now extends into the tabs, there is an increase in the effective cross-sectional area of the sample at the level of the tabs. Moreover, inside the main body of the tabs the helium is forced to be of a nearly uniform temperature, which also increases the apparent conductance of the sample. The use of the center-to-center spacing of the tabs would thus yield a conductivity which would be too large. The effective value of Δx for the low-temperature cell was determined by normalizing the data in the region of temperature overlap to agree with those obtained using the high-temperature cell. The effective spacing was found to be $\sim6\%$ shorter than the center-to-center distance. The magnitude of the correction seems reasonable bearing in mind that the diameter of the radial holes drilled into the tabs is $\sim20\%$ of the spacing. We also found, to within the precision of our data, that the normalizing factor was independent of density, even though the helium conductivity changed by a factor of about 2. Presumably, then any temperature dependence of the effective thermometer spacing is also very small.

For the low-temperature cell, the temperature-difference measurements were made by recording the thermometer-bridge ratios first with $\dot{Q}=0$ and then again with the heater current set to cause a ΔT of roughly $0.06T$. Both pairs of readings were obtained with the colder tab being regulated at the same temperature, using the thermometer on the cold tab and the heater located on the large heat exchanger (Fig. 1) in the control loop. The temperature difference between the tabs is then simply $T_{\text{bottom}}(\dot{Q})-T_{\text{bottom}}(0)$, which is insensitive to small differences in the temperature calibrations of the two thermometers. Approximately 90 min were required to regain a steady-state condition near 7 mK after changing T or Q. This time grew to several hours at 30 mK. Between 30 and 50 mK some of the data were obtained using an alternate procedure: The temperature of the large heat exchanger (rather than the cold tab) was maintained constant for each pair of readings. The ΔT generated by the heat flow was then $\Delta T_{\text{bottom}}-\Delta T_{\text{top}}$, and the mean temperature was $T_{\text{top}}(\dot{Q})+\frac{1}{2}\Delta T$.

All of the data for the high-temperature cell were obtained using this second method. The heater powers were now adjusted to cause a $\Delta T/T$ of ~0.12. With this apparatus, approximately 1 h was required to establish steady-state conditions over the complete temperature range.

D. Empty cell: Thermal conductivity of Cu_{70}-Ni_{30}

Before admitting ^{3}He to the high-temperature cell (Fig. 2), the thermal conductance of the Cu-Ni tube was measured. The density (8.94 g/cm^3) and the measured mass

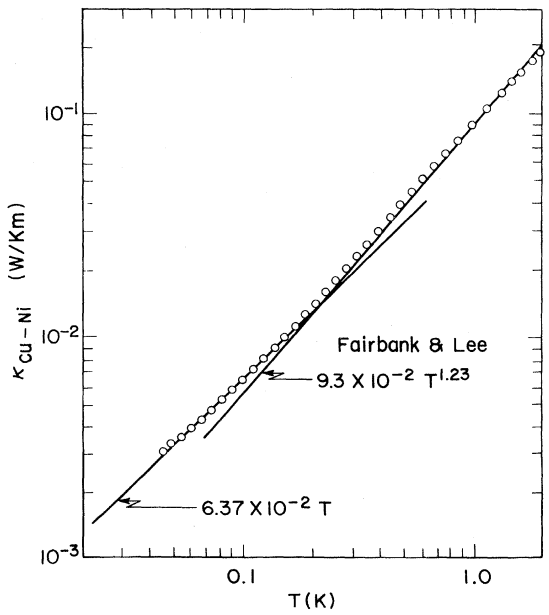

FIG. 3. Conductivity of Cu_{70}-Ni_{30}. Comparison is made with the work of Fairbank and Lee (Ref. 9).

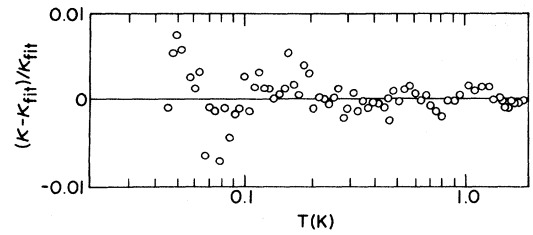

FIG. 4. Relative deviations from a least-squares fit of the Cu-Ni conductivity data. Above 100 mK the precision of the data is a few tenths of a percent.

per unit length of the tubing determined the cross-sectional area of the metal sample. Figure 3 shows the conductivity plotted on log-log scales. Below 200 mK, κ is approximately proportional to T; at higher temperatures the conductivity grows at a faster rate. The straight line associated with these higher-temperature data corresponds to the expression used by Fairbank and Lee[9] to describe their results between 0.3 and 4.0 K. The agreement in both magnitude and temperature dependence is excellent.

Empty-cell conductivity measurements could not be made using the low-temperature cell. This is because of the extremely long thermal time constants resulting from the coupling of the small conductance of the tube and the large thermal masses[1] of the melting-curve thermometers. However, the helium conductivity data for this cell could be accurately corrected for the shunting effect of the cylinder walls since the bodies of both cells were cut from the same length of Cu-Ni tubing. It was assumed that the κ remained linear in T down to the lowest temperatures.

The deviations of the Cu-Ni data from a least-squares polynomial fit (six terms) are plotted in Fig. 4 to show the precision of these measurements. Figure 5 shows the fraction of heat flowing through the cylindrical walls of the two cells for helium densities corresponding to $P\approx 0$ and 30 bars.

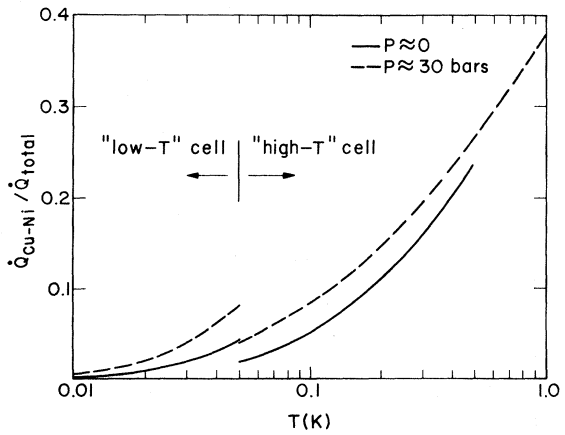

FIG. 5. Fraction of heat flowing through the Cu-Ni cylindrical walls of the two conductivity cells (Figs. 1 and 2). Curves are shown corresponding to the cells being filled with normal liquid ^{3}He at $P\approx 0$ and 30 bars.

III. RESULTS AND DISCUSSION

A. General results

The thermal conductivity of pure normal liquid ^{3}He was precisely measured for several molar volumes (listed in Table II) as well as over the temperature range from 7 mK to the temperature at which the expansion coefficient becomes positive. For $P\approx 0$ bars this occurs near 0.5 K and for $P\approx 30$ bars near 1.3 K. Because of the experimental considerations discussed in Sec. II A, the measurements were made using two different conductivity cells. The low-temperature cell was used to a maximum temperature of 50 mK; the high-temperature cell to a minimum temperature of about 40 mK.

All of the conductivity data are plotted in Fig. 6 with the different symbols referring to the two apparatuses. Consistent with theoretical expectations for this Fermi system, each string of data tends towards a T^{-1} temperature dependence at low temperature and roughly towards a $T^{1/2}$ dependence at high temperature. It is also observed that as the density increases the conductivity decreases. Figure 7 shows the data below 60 mK plotted on linear scales.

The pioneering work directed toward an understanding of the transport properties of normal liquid ^{3}He at $T=0$ is that of Abrikosov and Khalatnikov,[10] who derived the quasiparticle transport equation based on Landau Fermi-liquid theory. In doing so they also demonstrated that the quasiparticle interaction function does not appear explicitly in the equations and thus that the transport problem in the Fermi liquid is formally identical to that of the Fermi gas. The transport coefficients were given in terms of solutions to integral equations which were later solved exactly by Brooker and Sykes[11] and also by Højgaard Jensen *et al.*[12] The problem therefore reduces to determining the scattering amplitude for pairs of quasiparticles with momenta on the Fermi surface.

The solution for the thermal conductivity can be written in the form analogous to that from simple kinetic theory,

$$\kappa=\tfrac{1}{3}(C_V/V)v_F^2\tau_\kappa\,. \tag{2}$$

TABLE II. Molar volumes of the ^{3}He samples.

Sample	Pressure at 0.1 K (bar)	Molar volume (cm^3)	Temperature range (K)
1	0.12	36.675	0.007—0.05
2	4.60	32.826	0.007—0.05
3	10.16	30.333	0.007—0.05
4	20.23	27.650	0.007—0.05
5	29.29	26.273	0.007—0.04
6	0.10	36.701	0.05—0.5
7	4.60	32.824	0.05—0.6
8	10.20	30.319	0.05—0.8
9	20.20	27.656	0.05—1.0
10	29.98	26.172[a]	0.05—1.3

[a]Inferred from the solid nucleation temperature.

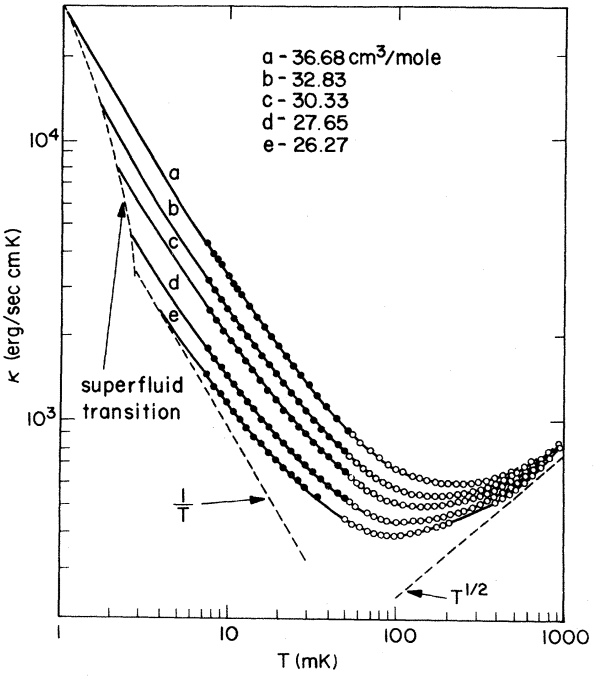

FIG. 6. Thermal-conductivity data for normal liquid ^{3}He on log-log scales. The solid and open circles represent data obtained using the cells shown in Figs. 1 and 2, respectively.

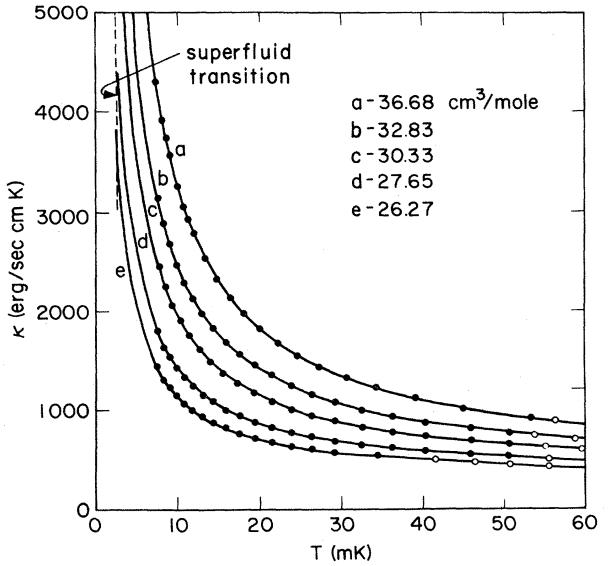

FIG. 7. Thermal-conductivity data below 60 mK plotted on linear scales. The solid and open circles represent data obtained using the cells shown in Figs. 1 and 2, respectively.

Here C_V is the molar specific heat at constant volume, V is the molar volume, v_F is the Fermi velocity, and τ_κ is the scattering time appropriate for thermal conductivity. The scattering time is proportional to T^{-2} at very low-temperatures as a consequence of the Pauli exclusion principle, which permits only particles in states near the Fermi level to scatter. At very low temperatures we also have

$$C_V/R = (\pi^2/2)(T/T_F) \tag{3}$$

and

$$v_F^2 = 2k_B T_F/m_3^* , \tag{4}$$

where R is the gas constant, and

$$T_F = (\hbar^2/2m_3^* k_B)(3\pi^2 N/V)^{2/3} . \tag{5}$$

It then follows that, in this regime, κ is inversely proportional to T.

For temperatures high compared to T_F, Boltzmann statistics apply, and kinetic theory gives the result that, for an ideal gas, $\kappa \propto (T/m_3)^{1/2}$. The data shown in Fig. 6 extend upward in temperature to only 1 K, which is of the order of T_F. Here the data are approaching density independence, but the temperature dependence differs from $T^{1/2}$. This is not surprising since the molar specific heat near 1 K also differs considerably from the classical value of $\frac{3}{2}R$.

Another notable feature of the data is that at very low temperatures the conductivity decreases with increasing ^{3}He density, contrary to the results[6] for dilute ^{3}He-^{4}He mixtures. In the latter case, the Fermi system is only slightly nonideal and τ_κ has only a weak density (i.e., concentration) dependence.[13] Consequently, κ is roughly proportional to ^{3}He density. The very different behavior of the pure liquid is a manifestation of the strong interactions experienced by the ^{3}He atoms.

B. Comparison with earlier measurements

Comparison with the $P \approx 0$ results from earlier experiments is made in Fig. 8, which shows the relative differences from the more-precise present measurements. It should be noted that in all of the previous experiments magnetic cooling was used, and, consequently, true steady-state conditions could not be achieved. This is an important consideration in these experiments because of the very long relaxation times encountered. As already discussed, the long times at very low temperatures are due to the large thermal boundary resistance, and at higher temperatures they are due to the small thermal diffusivity. These experiments also have the complication that a portion of the power generated in the tube heater goes toward increasing the temperature of the sample. Bearing in

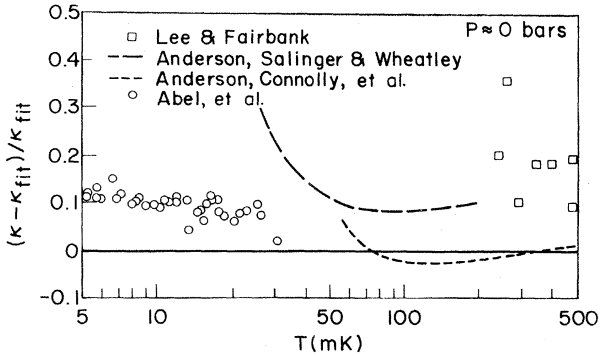

FIG. 8. Comparison of thermal-conductivity data obtained near $P = 0$ bars. $\kappa_{\rm fit}$ refers to Eqs. (6) and (7).

TABLE III. Best-fit parameters for Eqs. (6) and (7). The units for the conductivity and molar volume are erg/sec cm K and cm^3, respectively.

j	0	1	2
a_{0j}	$-4.188\,474\,6\times10^{1}$	1.926 283 9	
a_{1j}	$-1.854\,637\,9$	$2.369\,519\,0\times10^{-1}$	$-6.828\,475\,6\times10^{-3}$
a_{2j}	$4.361\,779\,2\times10^{-1}$	$-4.210\,167\,3\times10^{-2}$	$1.005\,022\,1\times10^{-3}$
a_{3j}	$-9.432\,829\,6\times10^{-2}$	$8.919\,626\,7\times10^{-3}$	$-2.090\,316\,5\times10^{-4}$
b_{-2j}	2.549 899 7	$-1.186\,190\,5\times10^{-1}$	$1.718\,778\,7\times10^{-3}$
b_{-1j}	$-1.486\,147\,2\times10^{2}$	7.217 632 9	$-7.543\,915\,7\times10^{-2}$
b_{0j}	$1.031\,123\,9\times10^{3}$	$-4.108\,463\,6\times10^{1}$	$6.818\,853\,4\times10^{-1}$
b_{1j}	$-3.374\,651\,7\times10^{3}$	$2.261\,261\,2\times10^{2}$	$-3.420\,780\,1$
b_{2j}	$2.591\,379\,2\times10^{3}$	$-1.457\,499\,8\times10^{2}$	2.138 964 3

mind the precision of the earlier data, and also the fact that the total systematic errors are estimated to be as large as 10%, the agreement is reasonable.

The largest amount of scatter occurs in the data of Lee and Fairbank[3] (open squares), which represent, however, the first conductivity measurements on normal liquid ^{3}He. The long-dashed curve corresponds to the smoothed results of Anderson, Salinger, and Wheatley.[4] These measurements extended to much lower temperatures and were the first to exhibit the increase in thermal conductivity with decreasing temperature, a characteristc of the Fermi-liquid regime. Thermal equilibrium was a serious problem in this experiment; presumably this explains the very large deviations from the present measurements at the lower temperatures.

The short-dashed curve shows the smoothed results of Anderson, Connolly, Vilches, and Wheatley,[5] who also made measurements under pressure. The agreement between these and the present data is within the few percent scatter in the earlier measurements, except near 60 mK, where the two sets of measurements diverge. This departure at the low-temperature end of their range may be related to the difficulties which they experienced with their carbon-resistance thermometers. It was reported that these problems prevented them from extending their measurements to lower temperatures.

The most-recent and lowest-temperature data (open circles) are due to Abel, Johnson, Wheatley, and Zimmermann.[6] Outside of the systematic differences, these values are also in quite good agreement with the present work. It is interesting that these deviations are similar in both magnitude and temperature dependence to the relative differences between the specific-heat measurements of Abel, Anderson, Black, and Wheatley,[14] and those reported in Ref. 1 (see Fig. 16 of this reference). These two pairs of experiments are based on the same respective types of thermometry. However, possible differences in the two temperature scales probably cannot be invoked to

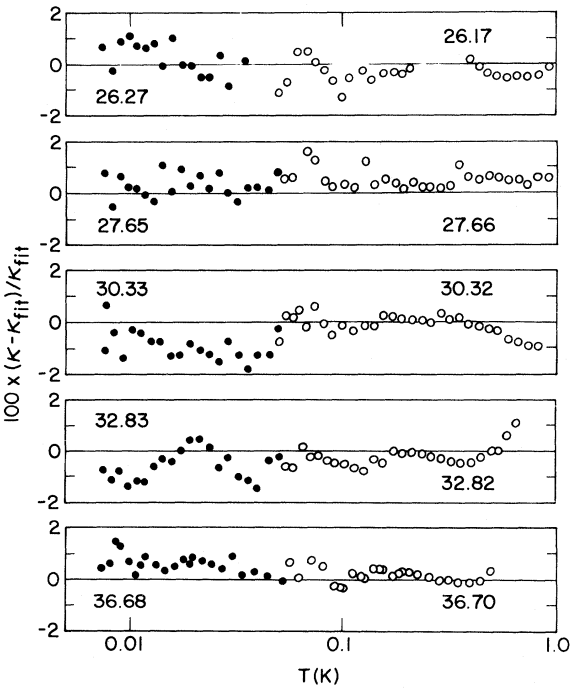

FIG. 9. Derivations from least-squares fits to the thermal-conductivity data. Equation (6) was used below 50 mK, and Eq. (7) above 50 mK. The numbers give the molar volume in cm^3. The closed and open circles correspond to data obtained with the apparatuses shown in Figs. 1 and 2, respectively.

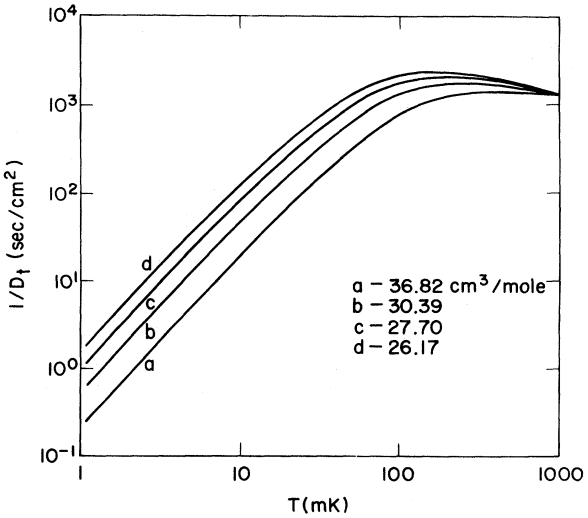

FIG. 10. Inverse of the thermal diffusivity plotted vs the temperature. The diffusivity was determined using Eqs. (6) and (7) for the thermal conductivity and Eqs. (7) and (8) of Ref. 1 for the specific heat.

entirely explain the discrepancies in both the thermal-conductivity and specific-heat experiments. If, for example, the two scales were simply related by a uniform shift, then the relative differences for the two types of measurements would be of opposite sign.

C. Empirical equations describing the conductivity data

The curves drawn through the conductivity data in Figs. 6 and 7 correspond to least-squares fits of the measured values, with both the temperature and molar volume as independent variables. Below 50 mK the fitting function was

$$\frac{1}{\kappa T}=\sum_{i=0} T^i\left[\sum_{j=0} a_{ij}V^j\right]^{-1}. \tag{6}$$

Above this temperature the fitting was performed using the expression

$$\kappa=\sum_{\substack{i=-2\\ j=0}} b_{ij}V^jT^i. \tag{7}$$

The best-fit parameters are listed in Table III, and the relative deviations are plotted in Fig. 9. The rms derivations are 1.0% and 0.5%, respectively. Some smoothed values of κ, along with other derived quantities, are tabulated in Table IV at several molar volumes corresponding to nominal sample pressures that are multiples of 5 bars.

The inverse of the thermal diffusivity, $D_t\equiv\kappa V/C_V$, is plotted in Fig. 10 for several molar volumes as well as against temperature using C_V from Ref. 1. Since l^2/Dt is approximately the thermal relaxation time for a sample of linear dimension l, Fig. 10 can be used directly to estimate these times. For $l\approx 1$ cm and $P\approx 0$ the thermal time constant is ~ 0.2 sec at 1 mK (neglecting boundary resistance), but ~ 1000 sec above 100 mK.

D. Zero-temperature results

The conductivity results extrapolated to $T=0$ are plotted as a function of molar volume in Fig. 11. The solid circles are from fits of the data obtained at each molar volume and at temperatures less than 50 mK using the function

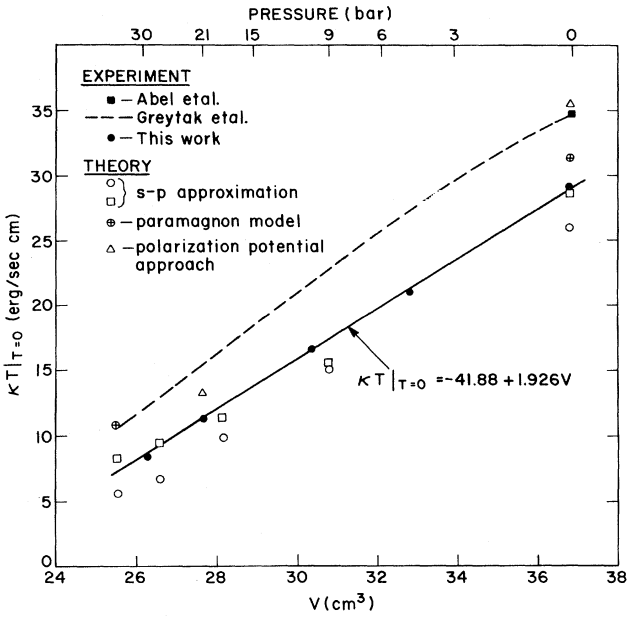

FIG. 11. Thermal conductivity of normal liquid ^{3}He at $T=0$ K. Details are given in the text.

$$1/\kappa T=a+bT+cT^n, \tag{8}$$

with $n=2$. Justification for this particular expression will be given in Sec. III E. We note that using $n=3$ or 4 worsened the fit and also considerably changed the b values; however, the leading term remained unchanged to within better than 2%. A curious finding is that, to within the precision of the measurements, $\kappa T\,|_{T=0}$ is a linear function of the inverse of the density. The straight line drawn in Fig. 11 comes from the more general fit, Eq. (6), in which the data at all densities were treated simultaneously. (Smoothed zero-temperature values are listed at several molar volumes in Table V.)

The solid square in Fig. 11 corresponds to the experi-

TABLE V. Smoothed zero-temperature parameters derived from the measured thermal conductivity. The quantities τ_κ and v_F are based on m_3^* values from Ref. 1. The quantity b is defined by Eq. (10).

P (bar)	V (cm^3/mol)	p_F (10^{-20} g cm/sec)	v_F (10^3 cm/sec)	κT (erg/sec cm)	$\tau_\kappa T^2$ (10^{-12} sec K^2)	b (cm sec/erg K)
0	36.84	8.28	6.00	29.08	0.391	−0.42
3	33.87	8.52	5.42	23.36	0.329	−0.60
6	32.07	8.67	5.04	19.89	0.291	−0.78
9	30.76	8.79	4.72	17.37	0.263	−0.97
12	29.71	8.89	4.47	15.35	0.241	−1.19
15	28.86	8.98	4.24	13.71	0.222	−1.42
18	28.13	9.06	4.03	12.30	0.206	−1.69
21	27.56	9.12	3.86	11.20	0.193	−1.96
24	27.06	9.18	3.71	10.24	0.181	−2.26
27	26.58	9.23	3.57	9.32	0.169	−2.63
30	26.14	9.28	3.44	8.47	0.158	−3.06
33	25.71	9.34	3.30	7.64	0.147	−3.62
34.36	25.54	9.36	3.24	7.31	0.143	−3.89

TABLE IV. Smoothed results for the thermal conductivity of normal liquid ^{3}He, and other derived quantities. The specific heat values needed for the computations were taken from Ref. 1. The molar volumes (V) and pressure (P) are in cm^3 and bar, respectively.

T (K)	v_F (10^3cm/sec)	κT (erg/sec cm)	$\tau_\kappa T^2$ (10^{-12} sec K^2)	$D_t T^2$ (cm^2/sec K^2)	T (K)	v_F (10^3 cm/sec)	κT (erg/sec cm)	$\tau_\kappa T^2$ (10^{-12} sec K^2)	$D_t T^2$ (cm^2/sec K^2)
		$V=36.82$, $P=0$					$V=28.89$, $P=15.0$		
0.000	6.00	29.0	0.391	4.69	0.000	4.24	13.8	0.223	1.34
0.005	6.00	30.8	0.415	4.98	0.005	4.25	15.1	0.245	1.47
0.010	6.01	32.7	0.439	5.28	0.010	4.27	16.6	0.267	1.63
0.015	6.03	34.5	0.462	5.60	0.015	4.31	18.2	0.290	1.79
0.020	6.05	36.4	0.485	5.93	0.020	4.36	19.8	0.312	1.98
0.025	6.09	38.2	0.507	6.26	0.025	4.43	21.5	0.333	2.17
0.030	6.13	40.1	0.528	6.61	0.030	4.50	23.1	0.353	2.38
0.035	6.18	42.0	0.549	6.98	0.035	4.58	24.8	0.372	2.61
0.040	6.23	43.8	0.568	7.35	0.040	4.67	26.5	0.390	2.84
0.045	6.30	45.7	0.586	7.74	0.045	4.77	28.2	0.406	3.09
0.050	6.37	47.6	0.604	8.16	0.050	4.88	29.9	0.421	3.35
		$V=32.59$, $P=5.0$					$V=27.70$, $P=20.0$		
0.000	5.15	20.9	0.302	2.67	0.000	3.90	11.5	0.197	1.00
0.005	5.16	22.5	0.325	2.88	0.005	3.91	12.8	0.218	1.11
0.010	5.17	24.2	0.348	3.10	0.010	3.94	14.2	0.240	1.24
0.015	5.20	25.9	0.371	3.34	0.015	3.98	15.6	0.262	1.39
0.020	5.23	27.7	0.393	3.59	0.020	4.04	17.2	0.284	1.55
0.025	5.28	29.4	0.415	3.86	0.025	4.11	18.8	0.306	1.72
0.030	5.33	31.3	0.437	4.13	0.030	4.19	20.4	0.326	1.90
0.035	5.39	33.1	0.457	4.42	0.035	4.28	22.0	0.344	2.10
0.040	5.46	34.9	0.476	4.73	0.040	4.38	23.6	0.360	2.30
0.045	5.54	36.7	0.494	5.05	0.045	4.49	25.2	0.375	2.52
0.050	5.62	38.6	0.511	5.39	0.050	4.60	26.7	0.388	2.74
		$V=30.39$, $P=10.0$					$V=26.17$, $P=30.0$		
0.000	4.63	16.7	0.256	1.83	0.000	3.44	8.5	0.159	0.63
0.005	4.64	18.1	0.278	1.99	0.005	3.45	9.7	0.180	0.72
0.010	4.66	19.7	0.300	2.18	0.010	3.48	11.0	0.203	0.82
0.015	4.70	21.3	0.323	2.37	0.015	3.53	12.4	0.225	0.93
0.020	4.74	23.0	0.345	2.58	0.020	3.59	13.8	0.247	1.06
0.025	4.79	24.7	0.367	2.81	0.025	3.67	15.3	0.269	1.20
0.030	4.86	26.5	0.388	3.05	0.030	3.75	16.8	0.288	1.35
0.035	4.93	28.3	0.407	3.30	0.035	3.85	18.3	0.305	1.51
0.040	5.01	30.0	0.426	3.57	0.040	3.96	19.6	0.319	1.67
0.045	5.10	31.8	0.443	3.85	0.045	4.07	20.9	0.330	1.82
0.050	5.20	33.6	0.459	4.14	0.050	4.19	22.1	0.339	1.98

mental work of Abel, Johnson, Wheatley, and Zimmermann,[6] already discussed in Sec. II B. The dashed curve was drawn using the smooth values tabulated in Ref. 15, which are based on the zero-pressure measurements of Abel *et al.*,[6] and on unpublished work under pressure by Greytak, Johnson, Paulson, and Wheatley. At small molar volumes the dashed curve differs from the present work by 40%, and at large molar volumes by only 20%. Thus the discrepancy cannot be attributed solely to the obvious possible errors, for example, in the thermometer spacing determinations. The fact that the two sets of data do not scale by a constant factor can be largely explained if the density dependence in the experiment of Greytak *et al.* was determined by simply measuring the conductivity at a given (but not-too-low) temperature. This is because the relative density dependence of κT grows with decreasing temperature (Sec. III E).

The open symbols plotted in Fig. 11 corresponds to theoretical values, all of which show reasonably good agreement with experiment in both magnitude and density dependence. In the s and p approximations of Dy and Pethick[16] it is assumed that only s and p waves contribute to the scattering. Consequently, the scattering amplitudes for pairs of particles with parallel and antiparallel spins can be written in terms of the Landau parameters $F_l^{s,a}$. The open circles are the s and p conductivities evaluated by Tešanović and Valls[17] neglecting Landau parameters with $l>1$ and using the values of F_0^s, F_0^a, and F_1^s tabulated in Ref. 1. F_1^a was determined using the forward-scattering sum rule,[18]

$$\sum_{l=0}^{\infty}(A_l^s+A_l^a)=0\,, \tag{9}$$

where

$$A_l^{s,a}=\frac{F_l^{s,a}}{1+F_l^{s,a}/(2l+1)}\,.$$

Again, only terms with $l\leq 1$ were retained. ($F_l^a=-0.42$ at $P=0$ bars; $F_1^a=-0.24$ at $P=27$ bars.) The open squares, which are in better agreement with the new measurements, are also s and p values computed[19] as above, but with F_1^a determined[1] using the coefficient of the $T^3\ln T$ correction to the low-temperature specific heat. ($F_1^a=-0.55$ at $P=0$ bars; $F_1^a=-0.99$ at 27 bars.) The circled pluses in Fig. 11 are conductivities determined using the paramagnon model. These values were taken from the review paper of Levin and Valls,[20] and were determined using the ^{3}He effective mass from Ref. 1. Also indicated (open triangles) are the results of recent theoretical work by Pfitzner and Wölfle.[21] These calculations are based on the polarization-potential approaches of Pines and Bedell,[22] and Aldrich and Pines,[23] but modified to explicitly incorporate exchange symmetry.

E. Finite-temperature behavior

The various theories discussed in the preceding sections are all ultimately based on the assumption that the quasiparticle scattering takes place on the Fermi surface, and therefore strictly apply only in the limit of zero temperature. At finite temperatures the energy transfer in quasiparticle collisions must be taken into account. Emery[24] has shown that this implies, as a general feature of Fermi systems, that τ_κ^{-1} is proportional to terms in T^2 and T^3, and consequently that $1/\kappa T$ has the limiting low-temperature form $a+bT$. Since the b coefficient multiplies T rather than T^2, as one might have presumed, there is an explanation for the rather large departures of κ from $1/T$ behavior observed (Fig. 6), even for a temperature very small compared to T_F. Figure 12 shows the experimental data plotted as $1/\kappa T$ vs T to explicitly demonstrate the consistency with the theoretically predicted behavior. The smooth curves through the data were drawn using Eq. (6) and the best-fit parameters given in Table III. The straight dashed lines are extrapolations of the inferred limiting temperature dependences. In Fig. 13 the slopes of these lines, that is, the extracted b coefficients, are plotted as a function of molar volume. Fitting the data obtained with $T<30$ mK at each molar volume, using the expression

$$1/\kappa T=a+bT+cT^2\,, \tag{10}$$

yielded the values shown by the open squares. Including data up to 60 mK and adding a term in T^3 to the fitting relation yielded the value shown by the open circles. The uncertainties indicated correspond to standard errors.

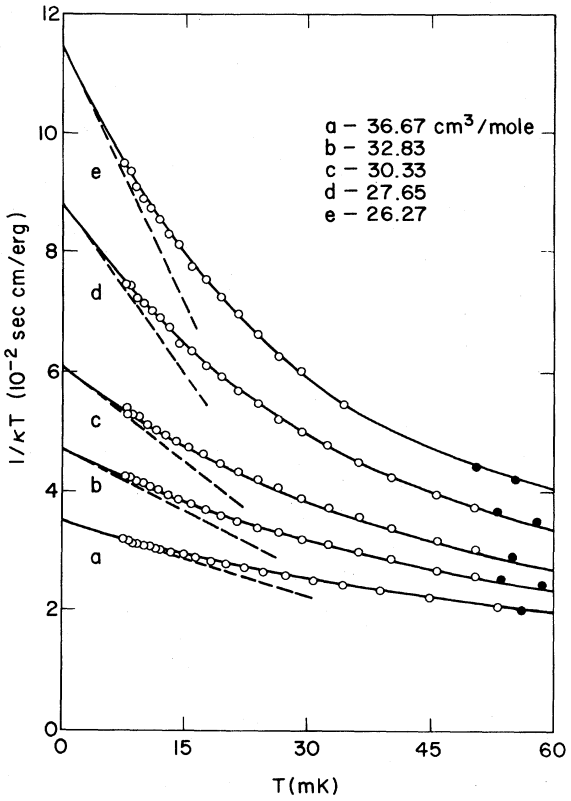

FIG. 12. Thermal-conductivity data plotted as $1/\kappa T$ vs T to demonstrate the consistency with theoretical predictions. The smooth curves were drawn using Eq. (6); the straight dashed lines are extrapolations of the very-low-temperature behavior. Data taken using the cells shown in Figs. 1 and 2 are indicated by the open and closed circles, respectively.

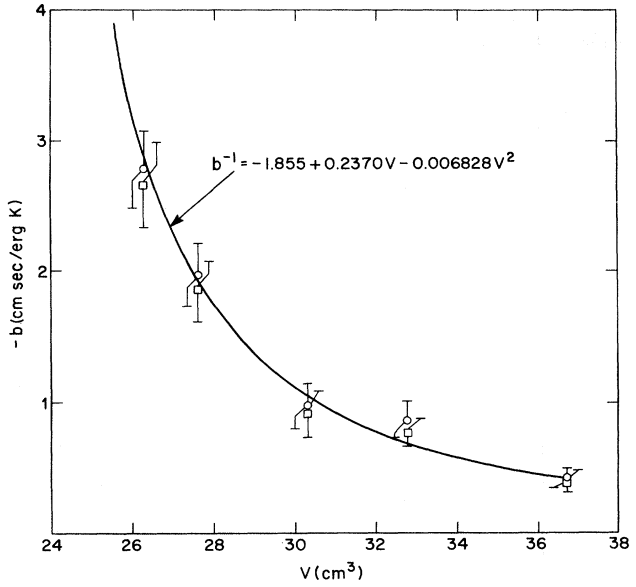

FIG. 13. Coefficient of the linear contribution to $1/\kappa T$ [see Eq. (10)].

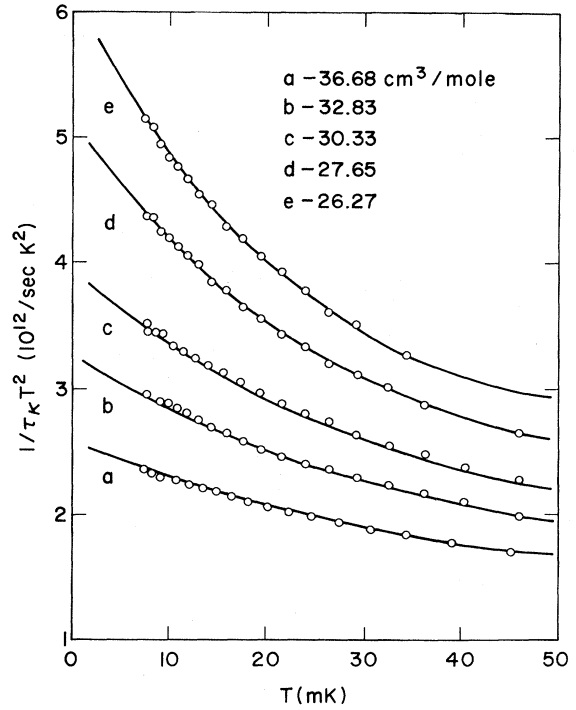

FIG. 14. Values of $1/\tau_\kappa T^2$ extracted from the thermal-conductivity data (see Sec. III F).

The smooth curve through the points corresponds to the fit (Sec. III C) in which the data at all densities were treated simultaneously.

At $P \approx 0$, comparison can be made with the results of Abel *et al.*,[6] who determined that $-b/a \approx 6.3$ K^{-1}. Our corresponding value is 12.2 K^{-1}. Since the data themselves differ (Fig. 8) quite uniformly by 10%, the explanation for the serious disagreement between these two numbers must be largely in the data analysis. In the older work, and consistent with the precision of those measurements, the data obtained below 30 mK were fitted using only the first two terms in Eq. (10). However, in the present work, the data have an order of magnitude greater precision and require the inclusion of the term in T^2 to adequately fit the data over the same temperature range. The curvature in the low-temperature data (Fig. 12), which increases with increasing density, then explains the larger $-b/a$ value estimated from the present measurements.

The experimentally determined, leading finite-temperature correction to the conductivity can, in principle, be compared with theoretical values using the expressions derived by Dy and Pethick.[16] These expressions, however, are not in analytic form and have not yet been evaluated using the Landau parameters of Ref. 1.

F. Scattering time at finite temperature

Thus far the analysis has been concerned directly with the quantity experimentally measured, i.e., the thermal, conductivity. However, the more fundamental parameter connected with this transport property is the scattering time τ_κ. In fact, it is the finite-temperature corrections to τ_κ which actually have been determined theoretically. Certainly, at sufficiently low temperatures C_V is proportional to T and there is no ambiguity in the relation between τ_κ and κ. Experimentally, it is observed, however, that the finite-temperature corrections to the specific heat are already detectable at temperatures of the order of 10 mK, particularly at the higher pressures. Consequently, at least part of the T^2 contribution to $1/\kappa T$ is attributable to the $T^3 \ln T$ contributions to C_V. We ask if it is not pos-

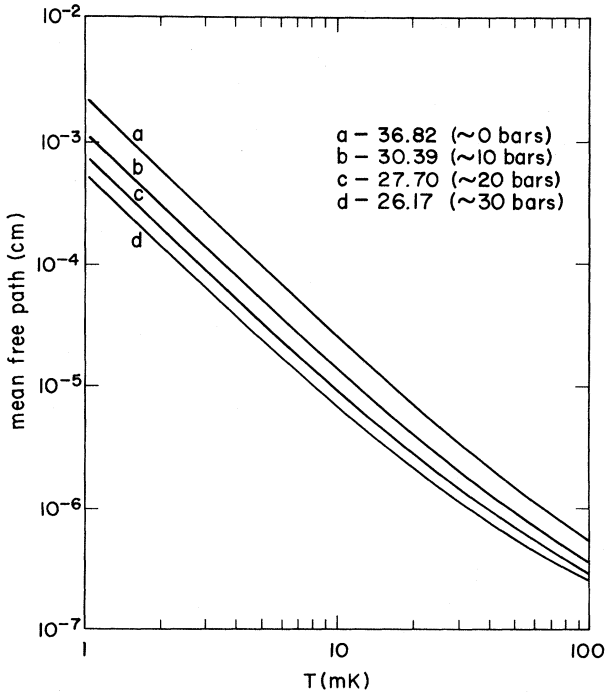

FIG. 15. Quasiparticle mean free path defined by the product of $\tau_\kappa(T)$ from Eq. (11) and $v_F(T)$ from Eq. (13).

TABLE VI. Parameters resulting from least-squares fits of $1/\tau_\kappa T^2$ extracted from thermal-conductivity and specific-heat (Ref. 1) data using Eq. (14). The parameter a_τ was not adjustable (see text).

V (cm^{3}mol)	a_τ (10^{12}/sec K^2)	b_τ (10^{12}/sec K^3)	c_τ (10^{12}/sec K^4)	Θ_τ (K)	rms deviations (%)
36.67	2.58	−36.2	−177.0	0.38	0.29
32.83	3.26	−46.9	−102.0	0.30	0.64
30.33	3.94	−68.3	−272.0	0.61	0.41
27.65	5.13	−120.0	−652.0	0.41	0.43
26.27	6.18	−172.0	−1130.0	0.33	0.44

sible that *most* of the T^2 contribution be from this source, and extract τ_κ values by combining the conductivity data with smoothed specific-heat results.

Rearranging Eq. (2), we have

$$\frac{1}{\tau_\kappa T^2}=\frac{v_F^2}{3V}\left[\frac{C_V}{T}\right]\left[\frac{1}{\kappa T}\right]. \tag{11}$$

The conversion from κ to τ_κ, therefore, would be straightforward were it not for the factor v_F^2; since the specific heat is not strictly proportional to T there is uncertainty in how to determine v_F at finite temperatures. According to recent theoretical work,[25–27] the deviation of the specific heat from a linear temperature dependence should be interpreted in terms of a temperature-dependent average effective mass. Referring to Eqs. (3) and (5), this mass can be defined by

$$m_3^*(T)=\frac{C_V}{RT}\frac{\hbar^2}{\pi^2 k_B}\left[\frac{3\pi^2 N}{V}\right]^{2/3}, \tag{12}$$

which leads to the expression

$$v_F(T)=p_F/m_3^*(T) \tag{13}$$

used in this analysis.

Figure 14 shows the inferred values of $1/\tau_\kappa T^2$ plotted against the temperature. Figure 15 shows the quasiparticle mean free path defined by $v_F(T)\tau_\kappa(T)$. In both figures the solid curves are based on the smooth conductivity values, Eq. (6).

The fact that curvature remains in the data as plotted in Fig. 14 means that higher-order contributions to $1/\tau_\kappa T^2$ are indeed important, even at relatively low temperatures. Although these terms have not been studied in detail theoretically, they are thought to be of the form $T^2 \ln T$. We have tested the data for consistency with this expectation by fitting the results obtained below 60 mK using the expression

$$1/\tau_\kappa T^2=a_\tau+b_\tau T+c_\tau T^2 \ln(T/\Theta_\tau) \tag{14}$$

The parameters b_τ, c_τ, and Θ_τ were adjustable; a_τ was fixed using values of $\kappa T \mid_{T=0}$ from Eq. (6) and $C_V/T \mid_{T=0}$ from Eq. (7) of Ref. 1. The best-fit parameters are listed in Table VI. It is interesting that Θ_τ has a value of about 0.4 K; from an analysis of the $T^2 \ln T$ contribution to C_V/T it was determined that the characteristic temperature ranged from 0.46 K at $P \approx 0$ bars to 0.22 K at $P \approx 30$ bars.

ACKNOWLEDGMENT

I am grateful to Paul A. Busch for his expert technical assistance.

[1] D. S. Greywall, Phys. Rev. B 27, 2747 (1983).
[2] D. C. Carless, E. H. Hall, and J. R. Hook, J. Low Temp. Phys. 50, 583 (1983).
[3] D. M. Lee and H. A. Fairbank, Phys. Rev. 116, 1359 (1959).
[4] A. C. Anderson, G. L. Salinger, and J. C. Wheatley, Phys. Rev. Lett. 6, 443 (1961).
[5] A. C. Anderson, J. I. Connolly, O. E. Vilches, and J. C. Wheatley, Phys. Rev. 147, 86 (1966).
[6] W. R. Abel, R. T. Johnson, J. C. Wheatley, and W. Zimmermann, Phys. Rev. Lett. 18, 737 (1967).
[7] D. S. Greywall and P. A. Busch, J. Low Temp. 46, 451 (1982).
[8] D. S. Greywall, Phys. Rev. B 23, 2152 (1981).
[9] H. A. Fairbank and D. M. Lee, Rev. Sci. Instrum. 31, 660 (1960).
[10] A. A. Abrikosov and I. M. Khalatnikov, Rep. Prog. Phys. 22, 329 (1959).
[11] G. A. Brooker and J. Sykes, Phys. Rev. Lett. 21, 279 (1968).
[12] H. Højgaard Jensen, H. Smith, and J. W. Wilkins, Phys. Lett. 27A, 532 (1968); Phys. Rev. 185, 323 (1969).
[13] E. P. Bashkin and A. E. Meyerovich, Adv. Phys. 30, 1 (1981).
[14] W. R. Abel, A. C. Andrews, W. C. Black, and J. C. Wheatley, Phys. Rev. 147, 111 (1966).
[15] J. C. Wheatley, Rev. Mod. Phys. 47, 415 (1975).
[16] K. S. Dy and C. J. Pethick, Phys. Rev. 185, 373 (1969).
[17] Z. Tešanović and O. T. Valls, J. Low Temp. Phys. 52, 31 (1983).
[18] D. Hone, Phys. Rev. 125, 1494 (1962).
[19] Z. Tešanović and O. T. Valls (private communication).
[20] K. Levin and O. T. Valls, Phys. Rep. 98, 1 (1983).
[21] M. Pfitzner and P. Wölfle, in *Quantum Fluids and Solids—1983 (Sanibel Island, Florida)*, Proceedings of a Symposium, edited by E. D. Adams and G. G. Ihas (AIP, New York, 1983), pp. 148–160.
[22] K. Bedell and D. Pines, Phys. Rev. Lett. 45, 39 (1980).

[23]C. H. Aldrich and D. Pines, J. Low Temp. Phys. 32, 689 (1978).
[24]V. J. Emery, Phys. Rev. 170, 205 (1968).
[25]G. E. Brown, C. J. Pethick, and A. Zaringhalam, J. Low Temp. Phys. 48, 349 (1982).
[26]S. Fantoni, V. R. Pandharipande, and K. E. Schmidt, Phys. Rev. Lett. 48, 878 (1982).
[27]B. L. Friman and E. Krotscheck, Phys. Rev. Lett. 49, 1705 (1982).